

# Spectral Mobile Mapping for Rapid Soil Diagnostics – Results of a Laboratory Based Feasibility Test

ANDRÁS JUNG<sup>1</sup> & MICHAEL VOHLAND<sup>1</sup>

*Zusammenfassung: Die Anwendungsmöglichkeiten der VIS-NIR Feldspektroskopie in der spektralen Bodendetektion sind bereits durch zahlreiche existierende Studien aufgezeigt worden. Die jeweils erzielten Ergebnisse (z.B. Schätzgenauigkeiten für verschiedene Bodenkonstituenten) sind unter anderem vom eingesetzten Spektrometer und der gewählten Messkonfiguration abhängig.*

*Neben den traditionellen Instrumenten („ground truthing“ mit Feldspektroradiometern, Sensoren auf Flugzeug- und Satellitenplattformen) gibt es in der Gelände- bzw. bodennahen Spektroskopie eine Reihe von Neuentwicklungen. So ist eine handgehaltene und bildgebende Spektralkamera ein fehlendes Element in der Spektraldatenkette. Eine solche Kamera kann Spektraldaten für eine Höhe von 100, 10 und 1 m generieren und somit zum Up- und Down-scaling von Modellen (Klassifikationen und Schätzmodellen) genutzt werden.*

*In diesem Paper wird der Einsatz einer nicht-scannenden Hyperspektralkamera (nomineller Spektralbereich 400-1000 nm) für ein „rapid soil sensing“ beschrieben. Die Spektralbilder wurden mit Punktspektren und nasschemischen Ergebnissen verglichen. Quantitativ bestimmt (PLSR und PLSR mit CARS-Variablenselektion) wurden die folgenden Zielgrößen: organischer Kohlenstoff (OC), heißwasserlöslicher Kohlenstoff (HWE-C) und Stickstoff (N).*

## 1 Introduction

Field reflectance spectroscopy has been widely used in proximal soil sensing for a long time (BEN-DOR & BANIN, 1995; SUDDUTH ET AL., 1989; UDELHOVEN ET AL. 2003; VISCARRA ROSSEL & MCBRATNEY, 1998). Typically, field reflectance spectra are collected by portable field spectrometers, which are often complemented by air- or spaceborne imaging spectrometers in upscaling missions. It is a complex and critical process to link spatial-spectral data at different scales since a field spectrometer collects 1D high-resolution spectra while an imaging spectrometer provides 2D data with less resolved spectra. Ground truthing (1D-diffuse reflectance spectroscopy) has always been an essential tool to link ground spectra to remotely sensed images (GOETZ 2009). The need on “point-pixel-image”-scaling is growing. SCHAEPMAN ET AL. (2009) reported that imaging spectroscopy has undergone an exponential growth in the last decades and there is a global hyperspectral data deficit and demand on converging mission concepts to provide more accurate hyperspectral data to the scientific communities. Behind the traditional instrument concepts (ground truthing field spectrometers, air- and spaceborne scanners), there are alternative developments in the ground-based and near-ground spectroscopy. However, ground-based imaging line-scanners are currently less widespread in ground truthing than portable field spectrometers. Even the VIS-NIR (400-1000 nm) spectral imaging is not preferred to rapid 1D-diffuse reflectance spectrometers. One reason for this is the time factor as operating a field line scanner on a tripod set-up is very time consuming compared to the use of a 1D-field spectrometer. One of the concepts to overcome this limitation is non-scanning hyperspectral

1) Geoinformatik und Fernerkundung, Institut für Geographie, Universität Leipzig, Johannisallee 19a, 04103 Leipzig; E-Mail: andras.jung@uni-leipzig.de; michael.vohland@uni-leipzig.de

imaging, which enables rapid (1ms) hyperspectral imaging in a hand-held mode (JUNG ET AL. 2013). This technique provides a missing part in the spectral data chain as it generates spectral imaging data in an altitude of less than 100, 10 or 1 m.

Due to the novelty there are no available references for non-scanning spectral cameras used in proximal soil sensing. We started some experiments in this field (with the UHD 285 hyperspectral frame camera) at the University of Leipzig in 2013 (JUNG ET AL. 2013). Although, there is a comprehensive list of studies and works conducted with line-scanners in soil spectroscopy. Recently, STEFFENS & BUDDENBAUM (2013) utilized a hyperspectral line-scanner from 400 to 1000 nm to determine the concentrations of carbon, nitrogen, aluminum, iron and manganese of a stagnic Luvisol profile under laboratory conditions. At airborne and spaceborne scales hyperspectral imaging sensors have been often used to analyze soil, vegetated and other kind of earth surfaces (STEVENS ET AL. 2010). Ground-based imaging spectroscopy has also been used in numerous studies using line-by-line-scanning principles (KURZ ET AL. 2012, VIGNEAU ET AL. 2011)

This paper describes how the non-scanning hyperspectral frame-camera technique may be utilized for rapid and real-time soil sensing. The studied sample set consisted of 40 soil samples, which were analyzed in the VIS-NIR spectral range up to 930 nm for their contents of organic carbon (OC), hot-water extractable carbon (HWE-C) and nitrogen (N).

## 2 Materials and Methods

### 2.1 Study site and field sampling

The soil sampling area is situated in the Northwest Saxon Basin (Geopark Muldenland), which is characterized by Permian bedrock geology (rhyolites and ignimbrites), Cretaceous-Tertiary weathering products (like Kaolin) and quaternary sediments (loess, Pleistocene terrace gravel).

Tab. 1: Soil texture of three selected soil samples (from loess and sandy moraine material)

	Sand (%)	Silt (%)	Clay (%)
Soil from loess	5	79	16
Soil from sandy loess	31	56	13
Soils over sandy moraine	82	9	6

Within the study area 40 randomly selected soil samples were taken on different agricultural fields from the very top layer. For the wet-chemical analysis, soil samples were sieved  $\leq 2$  mm, homogenised, air-dried and, for organic matter analyses, subsequently pulverized by grinding using an agate mortar. The total contents of OC and N were measured by gas chromatography after dry combustion at 1100°C with a EuroEA elemental analyser (HekaTech, Wegberg, Germany). Soil samples with possible free carbonate contents (pH values equal to or greater than 6.5) were pretreated to remove carbonate-C. Determination of HWE-C followed the method of KÖRSCHENS ET AL. (1998).

Tab. 2: Wet-chemical parameters of the studied soil samples

	<b>Mean</b>	<b>Min</b>	<b>Max</b>	<b>SD</b>
SOC (%)	1.54	0.62	4.31	0.74
HWE-C ( $\mu\text{g g}^{-1}$ )	652	306	1568	265
N (%)	0.145	0.048	0.377	0.068
Quotient $\text{C} \times \text{N}^{-1}$	10.9	8.5	18.0	2.2

## 2.2 1D- and 2D spectral data acquisition

For the acquisition of image data we used the UHD 285 hyperspectral frame camera. It provides 125 channels in a spectral range from 450 nm to 950 nm (sampling interval 4 nm). The aperture number (F) of the lens system is 13 with a focal length of 25 mm. A silicon CCD chip with a sensor resolution of  $970 \times 970$  pixel captures the full frame images. The dynamic image resolution is 14 bit. At normal sun light illumination, the integration time of taking one hyperspectral data cube is 1 ms. The camera is able to capture more than 15 spectral data cubes per second (cps) which facilitates hyperspectral video recording. The high-resolution imaging spectrometer coupled with the camera chip was designed and developed by ILM (Institute of Laser Technologies in Medicine and Metrology) at the University of Ulm and the Cubert GmbH. 1D-measurements were performed with an ASD (Analytical Spectral Devices, Boulder, Colorado) FieldSpec 4 Wide-Res spectroradiometer with an available spectral range from 350 to 2500 nm. The spectral resolution of this instrument is 3 nm at 700 nm and 30 nm at 1400/2100 nm.

The size of the calibrated reference panel (Zenith Polymer®) was 30 cm  $\times$  30 cm. For imaging and non-imaging measurements, the same white reference panel was used to keep the referencing process standardized.

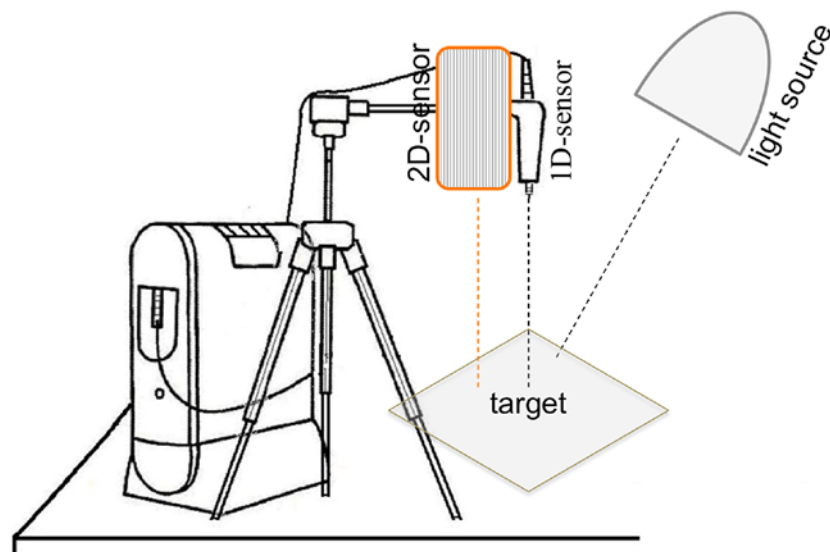


Fig. 1: Experimental set-up for 1D- and 2D spectral measurements in the lab

The soil samples were prepared at three different degrees of fineness (raw, sieved  $\leq 2$  mm and grinded) in order to minimize micro-shadowing and to maximize the spectral significance of the soil chemical components. The distance between sensor and soil sample was set to 35 cm in the nadir position, the illumination zenith angle was  $45^\circ$ . All samples were prepared on a reflection neutral plate (spectrally tested before) and covered, prior to the spectroscopic measurement, by a black passepartout (reflectance under 5 % over the entire spectral range from 400 to 2500 nm) with a window of  $20^\circ\text{cm} \times 20^\circ\text{cm}$ . The illumination source was an ASD Pro-Lamp model, that is tripod mountable for in-door laboratory diffuse reflectance measurements over the 350-2500 nm region.

For the data collection both spectrometers were mounted on a single tripod. After each measurement the sample was rotated by  $90^\circ$ , so that each sample was archived with 4 spectra. The spectra were pre-processed by ViewSpec (ASD software) and exported as mean spectra for the subsequent statistical analysis. The same measurement scheme was followed for the 2D-reflectance measurements. The native hyperspectral data cube was converted into bsq format and processed by the image analysis software ENVI (Exelis Visual Information Solutions).

2D-reflectance data (hyperspectral data cube) was calculated by an image mean operator that transformed the pixel spectra data into one mean spectrum. The mean image spectra were then exported as ASCII files for further statistical analysis.

### 2.3 Preprocessing of the spectral data

The spectral resolution of both datasets was adjusted prior to the statistical comparisons. In detail, both sets were reduced to 458-930 nm and spectrally resampled to the 4 nm resolution of the native image spectra. From this, 119 spectral dimension resulted for both the 1D reflectance vectors and the 2D image pixels. Additionally, spectra were transformed to absorbance spectra by  $\log(\text{reflectance}^{-1})$  and then transformed by the standard normal variate approach which is assumed to effectively remove the multiplicative interferences of scatter and particle size.

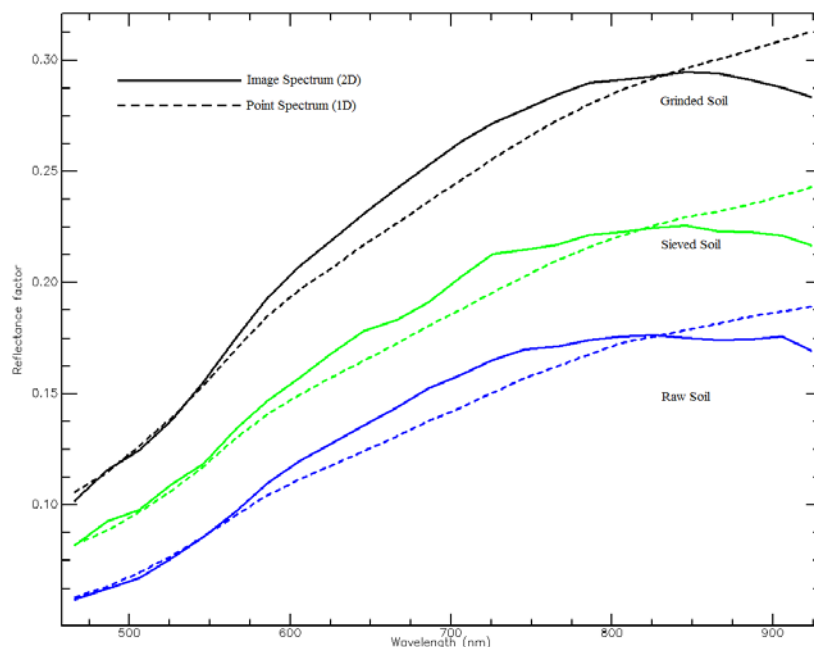


Fig. 2: 1D- and 2D reflectance curves after spectral resampling for raw, sieved and grinded soil samples captured by the hyperspectral camera (2D) and the ASD field spectrometer (1D)

## 2.4 Statistical methods

WOLD ET AL. (2001) published a comprehensive paper on the Partial Least Squares Regression (PLSR) which is mostly used in the field of chemometrics. PLSR is similar to principal component regression (PCR), as both employ statistical rotations to overcome the problems of high-dimensionality and multicollinearity. Different from PCR, PLSR maximises the covariance between the spectral matrix (X) and the chemical concentration matrix (Y) by accomplishing eigendecomposition of both matrices; the objective is to predict the information in Y as precisely as possible. To calibrate a PLSR model for each constituent, the optimum number of latent variables was identified by performing a leave-one-out cross-validation; the minimum root mean squared error (RMSE) in the cross-validation was used as decision criterion (with a predefined maximum of ten latent variables).

Many studies have shown that more accurate calibration models may be achieved by selecting the most informative spectral variables instead of using the full spectrum. For this purpose, we used the CARS (competitive adaptive reweighted sampling) approach, which was combined with PLSR to CARS-PLSR. For a detailed description of the CARS procedure please refer to LI ET AL. 2009. Briefly, it uses two successive steps of wavelength selection in a series of Monte Carlo sampling runs: In a first step, an exponentially decreasing function is used for an enforced removal of wavelengths with relatively small PLS regression coefficients. In a second step, an adaptive reweighted sampling of variables is employed to further eliminate wavelengths in a competitive way. In this step, random numbers are generated to pick variables; the probability of each spectral variable to be kept depends on its weight (calculated from the respective PLS regression coefficient).

To assess the accuracy of the multivariate calibration, we used the residual prediction deviation (RPD, defined as the ratio of standard deviation of the reference values to standard error of the cross-validated estimates), the coefficient of determination ( $R^2$ ), the root mean squared error (RMSE) and the percentage RMSE ( $\text{pRMSE} = \text{RMSE} \times \text{measured arithmetic mean}^{-1}$ ). Obtained accuracies (cross-validated values) were evaluated following the guideline of SAEYS ET AL. (2005) (Tab. 3): RPD and  $R^2$  values greater than 3.0 or 0.90, respectively, are considered to be indicative of an excellent prediction, whereas values from 2.5 to 3.0 (RPD) and 0.82 to 0.90 ( $R^2$ ) denote a good prediction. Approximate quantitative predictions are indicated by RPD values between 2.0 and 2.5 and  $R^2$  values in the range from 0.66 to 0.81. The possibility to distinguish between high and low values is revealed by values between 1.5 and 2.0 (RPD) and 0.50 and 0.65 ( $R^2$ ). Unsuccessful predictions have RPD or  $R^2$  values lower than 1.5 or 0.50, respectively.

Tab. 3: Prediction accuracies after SAEYS ET AL. (2005)

<b>Goodness</b>	<b>RPD</b>	<b><math>R^2</math></b>
Excellent	> 3.0	> 0.90
Good	> 2.5-3.0	0.82-0.90
Approximative quantitative	> 2.0-2.5	0.66-0.81
Possibility do distinguish between high and low values	1.5-2.0	0.50-0.65
Not suitable	< 1.5	< 0.50

### 3 Results

All cross-validated results are summarized in Tab. 4. In total, the highest accuracies were obtained with 1D full range spectra, which is in accordance with the general soil spectroscopic approach that considers the SWIR domain (1300-2500 nm) to be essential for OC and N spectral mapping. Excellent results were obtained with CARS-PLSR for OC (raw samples) and N (raw and grinded samples); for HWE-C, which represents a comparatively small labile carbon pool, results were slightly worse (good predictions); for this C pool, indirect VIS-NIR responses triggered by OC seem to be probable.

With a limited spectral range from 458 to 930 nm, accuracies obtained from the multivariate calibrations dropped distinctly. Best results (“good”) were obtained for OC (grinded samples, ASD and image spectra, both with CARS-PLSR) and HWE-C (grinded samples, from image spectra with CARS-PLSR).

For sieved samples, which are a bit more similar to in-situ conditions than grinded samples, best results were retrieved for OC from ASD spectra (full and limited range, in both cases “good” related to  $R^2$ ) and N from full range ASD spectra (“good” related to  $R^2$ ).

In contrast to a 1D-spectrometer, which performs spatially integrated measurements over the complete ground projected field of view, a frame camera captures micro-areas (pixels) that are much smaller in size. However, in our approach the spectral data cube was converted into a 1D-measurement in the post-processing as we averaged the entire image. This approach was helpful to clarify the comparability to pruned 1D-spectra and to show the usability of the image spectra for the quantitative approach (in fact, results were comparable or slightly worse especially for grinded samples). Further analyses without averaging the image spectra will be conducted to see which parts of the image would possibly provide a better match with 1D-spectra.

Grinded or sieved samples represent untypical situations for field surveys. Thus, further field measurements under natural solar conditions are needed to clarify the field suitability of the hyperspectral frame camera.

With respect to the statistical approaches, the CARS procedure has been shown to work effectively with respect to the parsimony of the statistical models (i.e. a reduced number of latent variables) and the obtained estimation accuracies. However, these results were obtained in cross-validations. The CARS procedure should thus be further examined with a larger number of soil samples using separate calibration and validation sets.

#### Acknowledgement

Our special thanks go to Cubert GmbH that made it possible to use and test the hyperspectral frame camera, by name to Rainer Graser and Dr. René Michels. CARS calculations were carried out using the freely available CARS package (Copyright Hongdong Li, 2011; <http://code.google.com/p/carspls/>).

Tab. 4: Cross-validated results from field spectrometer data (1D) and image mean spectra (2D) for raw, sieved and grinded soils; l.v.: number of latent variables (for CARS-PLS averaged from 50 runs); cv: leave-one-out cross-validation

Spectral dimension	Soil preparation level	Model	OC				N				HWE-C			
			l.v.	R <sup>2</sup> <sub>cv</sub>	RPD <sub>cv</sub>	pRMSE <sub>cv</sub>	l.v.	R <sup>2</sup> <sub>cv</sub>	RPD <sub>cv</sub>	pRMSE <sub>cv</sub>	l.v.	R <sup>2</sup> <sub>cv</sub>	RPD <sub>cv</sub>	pRMSE <sub>cv</sub>
1D 402-2398 nm 500 variables	raw	PLS	9	0.73	1.94	0.25	9	0.72	1.89	0.26	8	0.61	1.58	0.26
		CARS-PLS	8.2	0.93	3.85	0.13	8.0	0.91	3.30	0.15	7.2	0.86	2.73	0.15
	sieved	PLS	6	0.65	1.66	0.29	6	0.64	1.66	0.29	7	0.51	1.37	0.30
		CARS-PLS	6.0	0.84	2.49	0.19	6.0	0.84	2.49	0.19	6.0	0.72	1.91	0.21
	grinded	PLS	9	0.73	1.90	0.25	9	0.75	2.02	0.24	10	0.63	1.58	0.26
		CARS-PLS	6.7	0.88	2.93	0.16	7.3	0.92	3.53	0.14	8.2	0.88	2.86	0.14
1D 458-930 nm 119 variables	raw	PLS	7	0.41	1.28	0.37	10	0.34	1.19	0.41	7	0.43	1.28	0.32
		CARS-PLS	6.2	0.77	2.08	0.23	8.0	0.78	2.09	0.23	5.6	0.70	1.84	0.22
	sieved	PLS	9	0.63	1.64	0.29	8	0.45	1.34	0.36	9	0.64	1.64	0.25
		CARS-PLS	8.4	0.82	2.37	0.20	8.0	0.77	2.09	0.23	7.8	0.77	2.14	0.19
	grinded	PLS	10	0.66	1.73	0.28	10	0.49	1.38	0.35	9	0.56	1.49	0.27
		CARS-PLS	9.2	0.85	2.61	0.18	8.5	0.79	2.17	0.22	7.5	0.71	1.88	0.22
2D 458-930 nm 119 variables	raw	PLS	3	0.38	1.27	0.38	4	0.30	1.19	0.40	6	0.39	1.27	0.32
		CARS-PLS	3.5	0.49	1.42	0.34	3.0	0.42	1.33	0.36	4.1	0.58	1.56	0.26
	sieved	PLS	7	0.59	1.57	0.31	7	0.54	1.47	0.33	7	0.54	1.45	0.28
		CARS-PLS	6.5	0.72	1.89	0.25	6.7	0.70	1.83	0.26	5.6	0.62	1.63	0.25
	grinded	PLS	10	0.65	1.70	0.28	8	0.60	1.58	0.30	10	0.65	1.67	0.24
		CARS-PLS	8.4	0.84	2.49	0.19	7.1	0.75	2.01	0.24	8.9	0.83	2.45	0.17

excellent	good
-----------	------

## Literature

- BEN-DOR, E. & BANIN, A., 1995: Near-infrared analysis as a rapid method to simultaneously evaluate several soil properties. *Soil Sci. Soc. Am. J.*, **59**, S. 364-372.
- GOETZ, A.F.H., 2009: Three decades of hyperspectral remote sensing of the Earth: A personal view. *Remote Sens. Environ.*, **113**, S. 5-16.
- JUNG, A., VOHLAND, M., HEINRICH, J., MICHELS, R. & GRASER, R. 2013: Soil analysis with hyperspectral data – an experiment with a hyperspectral frame camera and VIS-NIR spectrometers. 8th EARSeL SIG Imaging Spectroscopy Workshop Nantes, France 8 – 10 April 2013.
- KÖRSCHENS, M., WEIGEL, A. & SCHULZ, E. 1998: Turnover of Soil Organic Matter (SOM) and Long-Term Balances – Tools for Evaluating Sustainable Productivity of Soils. *Z. Pflanz. Bodenkunde*, **161**, S. 409-424.
- KURZ, T.H., BUCKLEY, S. J. & HOWELL, J. A., 2012: Close range hyperspectral imaging integrated with terrestrial lidar scanning applied to rock characterisation at centimetre scale. *International Archives of the Photogrammetry, Remote Sensing and Spatial Information Sciences*, Volume XXXIX-B5, 2012 XXII ISPRS Congress, 25 August – 01 September 2012, Melbourne, Australia
- LI, H., LIANG, Y., XU, Q. & CAO, D., 2009: Key wavelengths screening using competitive adaptive reweighted sampling method for multivariate calibration. *Anal. Chim. Acta* **648**, S. 77-84.
- SAEYS, W. MOUAZEN, A.M. & RAMON, H., 2005: Potential for onsite and online analysis of pig manure using visible and near infrared spectroscopy. *Biosyst. Eng.*, **91**, S. 393-402.
- SCHAEPMAN, M.E., USTIN, S.L., PLAZA, A.J., PAINTER, T.H., VERRELST J. & LIANG, S., 2009: Earth system science related imaging spectroscopy – An assessment. *Remote Sens. Environ.*, **113**, S.123-137.
- STEFFENS, M. & BUDDENBAUM, H., 2013: Laboratory imaging spectroscopy of a stagnic Luvisol profile – High resolution soil characterisation, classification and mapping of elemental concentrations. *Geoderma*, **195–196**, S. 122-132.
- STEVENS, A., UDELHOVEN, T., DENIS, A., TYCHON, B., LIOY, R., HOFFMANN, L. & VAN WESEMAEL, B., 2010: Measuring soil organic carbon in croplands at regional scale using airborne imaging spectroscopy. *Geoderma*, **158**, S. 32-45.
- SUDDUTH, K.A., HUMMEL, J.W., FUNK, R.C., 1989: NIR soil organic matter sensor. *ASAE-Paper* **89-1035**.
- UDELHOVEN, T., EMMERLING, C. & JARMER, T., 2003: Quantitative analysis of soil chemical properties with diffuse reflectance spectrometry and partial-least-square regression: A feasibility study. *Plant Soil*, **251**, S. 319-329.
- VIGNEAU, N., ECARNOT, M., RABATEL, G. & ROUMET, P., 2011: Potential of field hyperspectral imaging as a non destructive method to assess leaf nitrogen content in wheat. *Field Crop Res.*, **122**, S. 25-31
- VISCARRA ROSSEL, R. A., & MCBRATNEY, A.B., 1998: Laboratory evaluation of a proximal sensing technique for simultaneous measurement of soil clay and water content. *Geoderma* **85**, 19–39.
- WOLD, S., SJÖSTRÖM, M. & ERIKSSON, L., 2001: PLS-regression: a basic tool of chemometrics. *Chemom. Intell. Lab. Syst.*, **58**, S. 109–130.